PROCEEDINGS OF SPIE

Evaluation of posterior porcine sclera elasticity <i>in situ</i> as a function of IOP

Achuth Nair, Chen Wu, Manmohan Singh, Chih Hao Liu, Raksha Raghunathan, et al.

SPIE.

Evaluation of Posterior Porcine Sclera Elasticity *in situ* as a function of IOP

Achuth Nair[a], Chen Wu[a], Manmohan Singh[a], Chih Hao Liu[a], Raksha Raghunathan[a], Jennifer Nguyen[a], Megan Goh[a], Salavat Aglyamov[b], and Kirill V. Larin[a,c,d,*]

[a]Department of Biomedical Engineering, University of Houston, Houston, TX, USA; [b]Department of Mechanical Engineering, University of Houston, Houston, TX, USA; [c]Interdisciplinary Laboratory of Biophotonics, Tomsk State University, Tomsk, Russia; [d]Molecular Physiology and Biophysics, Baylor College of Medicine, Houston, TX, USA

*klarin@uh.edu; Phone: 1 832 842-8834; Fax: 1 713 743-0226

ABSTRACT

The biomechanical properties of the sclera could provide key information regarding the progression and etiology of ocular diseases. For example, an elevated intraocular pressure is one of the most common risk factors for glaucoma and can cause pathological deformations in the tissues of the posterior eye, such as the sclera, potentially damaging these vital tissues. Previous work has evaluated scleral biomechanical response to global displacements with techniques such as inflation testing. However, these methods cannot provide localized biomechanical assessments. In this pilot work, we induce low amplitude (< 10 μm) elastic waves using acoustic radiation force in posterior scleral tissue of fresh porcine eyes (n=2) *in situ*. The wave propagation induced using an ultrasound transducer was detected across an 8 mm region using a phase-sensitive optical coherence elastography system (PhS-OCE). The elastographic measurements were taken at various artificially controlled intraocular pressures (IOP). The IOP was pre-cycled before being set to 10 mmHg for the first measurement. Subsequent measurements were taken at 20 mmHg and 30 mmHg for each sample. The results show an increase in the stiffness of the sclera as a function of IOP. Furthermore, we observed a variation in the elasticity based on direction, suggesting that the sclera has anisotropic biomechanical properties. Our results show that OCE is an effective method for evaluating the mechanical properties of the sclera, and reveals a new area for our future work.

Keywords: sclera, eye, ocular biomechanics, tissue biomechanical properties, Young's modulus, elastography, optical coherence elastography, ophthalmology

1. INTRODUCTION

The sclera is a critical load-bearing component of the eye-globe that extends from the cornea to the optic nerve and protects ocular components from mechanical deformation from external or internal forces, e.g. intraocular pressure (IOP)[1]. Several ocular pathologies, such as glaucoma and myopia, have been associated with alterations in the biomechanical properties of the sclera [2-5]. For example, it has been well established that myopia is produced by axial extension of the eye globe caused by changes in the scleral elasticity [4]. Severe cases such as high myopia are characterized by scleral thinning and localized ectasia of the posterior sclera [4]. Additionally, elevation in intraocular pressure (IOP) is one of the most common risk factors for glaucoma [6] and can cause pathological deformations in vital tissues in the posterior eye, damaging these tissues and reducing vision quality [6]. Thus, evaluating scleral biomechanical properties could potentially provide key information in understanding and assessing ocular disease etiology and progression.

Previous studies evaluating scleral biomechanical properties have largely focused on mechanical testing [7-9], inflation studies [10-12], atomic force microscopy (AFM) [13], computational modeling [14-16], and scattering-based imaging [5, 17]. These methods do provide important information about the biomechanical properties of the sclera, but each has its limitations. Mechanical testing generally involves mechanical evaluation of excised scleral strips. Elasticity measured with this method does not consider the whole eye-globe configuration or natural physiological effects like IOP on the sclera. AFM, on the other hand, cannot comfortably be used *in vivo*, especially for tissue that are difficult to access, such

as the sclera. Computational modeling can provide important information about the mechanical properties of the sclera. However, modeling is limited in accuracy by the measurements used for validation. Scattering-based methods like x-ray scattering and small-angle light scattering are effective for evaluating the collagen fibril orientation, but do not provide information regarding the macroscale effect of fibril orientation on tissue mechanical properties. Inflation testing usually maintains the whole eye-globe configuration and utilizes the IOP to induce deformations that are detected using imaging methods such as electronic speckle pattern interferometry [11, 18]. However, the strain measurements obtained using these methods often cannot be translated into quantitative biomechanical properties. Moreover, the large scale deformations that are induced limit the measurement resolution and often induce non-linear effects, which are difficult to assess. Considering the limitations of these established methods, a technique that could quantitatively evaluate biomechanical properties of the sclera *in vivo* would be a powerful tool for understanding the role of the biomechanical properties of tissues in the posterior eye on various ocular pathologies.

Elastography is a technique that was developed in the 1990s to assess the mechanical properties of tissues by detecting mechanical displacements with an imaging modality such as magnetic resonance imaging or ultrasound [19, 20]. While magnetic resonance elastography and ultrasound elastography have previously been used to evaluate scleral biomechanical properties [21, 22], the large displacement amplitudes needed for detection and the limited spatial resolution of the parent imaging modality of these techniques limits their effectiveness for small, relatively thin tissues like the sclera.

Optical coherence elastography (OCE) is an emerging technique that utilizes the high spatial resolution of optical coherence tomography (OCT) to obtain micrometer scale resolution [23] and sub-nanometer scale displacement sensitivity with phase-sensitive techniques [24]. The high resolution and highly sensitive nature of OCE makes it an effective tool to evaluate the elasticity of a sample with localized displacements. OCE has been previously used to evaluate the mechanical properties of ocular tissues such as the cornea and the lens [25-27]. In this work, we use acoustic radiation force to induce elastic waves in the sclera of *in situ* porcine eye-globes [27]. OCE measurements were taken at three random positions to examine the elasticity of the posterior sclera at various artificially controlled IOPs [28, 29]. Our results demonstrate the potential of OCE to quantitatively determine the elasticity of sclera.

2.   MATERIALS AND METHODS

Fresh porcine eyes in the whole eye-globe configuration (n=2) were positioned in a custom eye holder to facilitate IOP control and limit sample motion. The eye-globe was immersed in 0.9% saline to prevent tonicity from affecting the structural integrity of the sample. The eye-globe was cannulated in the holder to control IOP using a home-built closed-loop controller [30]. The eye-globe was pre-conditioned by cycling the IOP from 5 to 30 mmHg. OCE measurements were then taken at 10, 20, and 30 mmHg.

The US-OCE system utilized in this work consists of an ultrasound transducer with a 3.5 MHz central frequency coupled with a phase-sensitive spectral domain OCT system. Further details on the system can be found in our previous works [27]. Briefly, our SD-OCT system consists of a superluminescent diode light source with an 840 nm wavelength and a ~49 nm bandwidth. Axial and lateral resolution of the OCT system was measured as 6 μm and 8 μm in tissue, respectively. The system had a measured displacement sensitivity of ~2 nm, and was set at an A-line acquisition speed of 25 kHz. A 3.5 MHz sinusoidal wave generated by a function generator was amplified using a 50 dB power amplifier and drove the ultrasound transducer, which induced low amplitude (<10 μm) displacements in the tissue. A system schematic is shown in Figure 1.
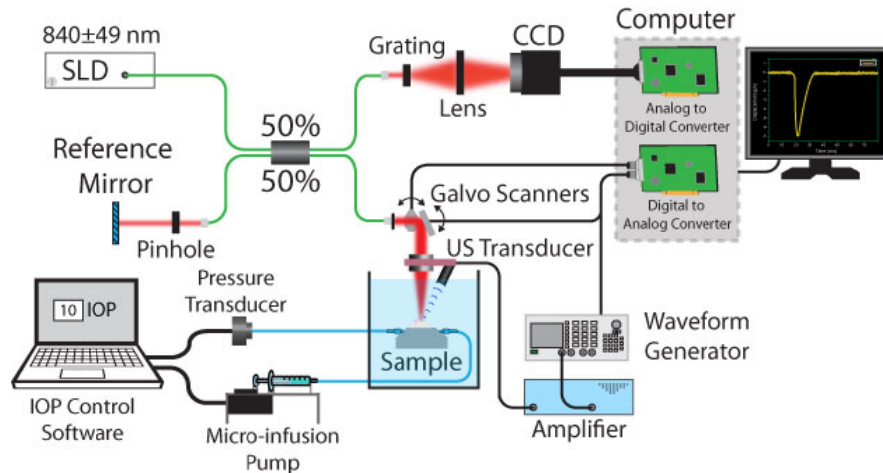
Figure 1: Schematic of the OCE system and experimental setup used to measure the biomechanical properties of the sclera.

The displacement was induced approximately 5 mm away from the optic nerve head. M-mode images were taken at 251 positions along an 8 mm linear scan along the sclera tissue, with the excitation centered along the linear scan [28]. The velocity of the acoustic radiation force induced surface wave was calculated by linearly fitting the wave propagation distances to the corresponding propagation delay from the original excitation position to the position where the wave attenuated, on each side of the excitation. Wave velocity was translated to elasticity using the surface wave equation [31]. It should be noted here that surface wave equation can only estimate the Young's modulus of tissues and more sophisticated analytical and computational models must be used in order to provide more accurate values of tissue elasticity and viscosity [32-36].

3. RESULTS

Figure 2 shows a typical OCT structural image of the sample, indicating regions used to calculate the wave velocity. Since the excitation was at the middle of the scan region, two directional assessments were made at once. Wave velocity was calculated from near the excitation position, to a position approximately 4 mm away from the excitation where the elastic wave could no longer be distinguished from the noise.
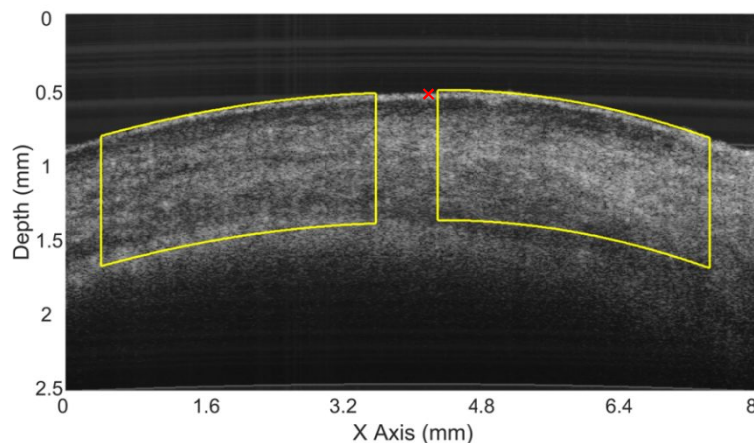

Figure 2: OCT structural image of a typical sample. The yellow boxes indicate the elastic wave calculation regions, and the red cross indicates the ultrasound induced excitation position.

Figure 3a and 3b shows the average sample group velocity, and the Young's modulus as estimated by the surface wave equation, for three different IOPs. As the IOP increased, the IOP-wise average Young's modulus increased from 1.7±0.6 MPa at 10 mmHg, to 2.6±1.0 MPa at 20 mmHg, and finally to 3.3±0.4 MPa at 30 mmHg. Figure 3c shows the averaged directional assessment of group velocity.
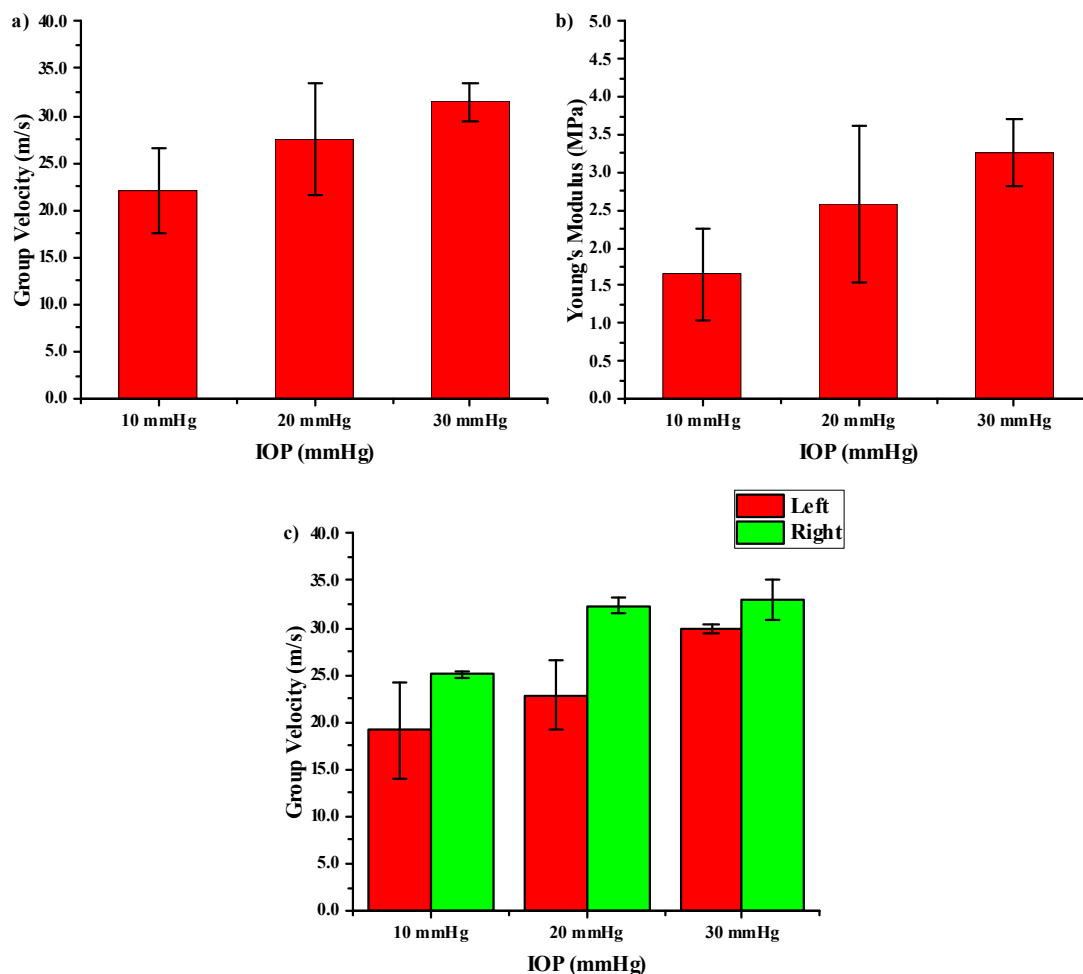

Figure 3: a) The mean IOP-wise average group velocity for each sample. The error bars are the sample-wise standard deviation. b) The mean IOP-wise average Young's Modulus for each sample, estimated from the group velocity by the surface wave equation. The error bars are the sample-wise standard deviation. c) The directional assessment of group velocity, where "left" and "right" correspond to the direction from the excitation position. The error bars are the depth-wise standard deviation.

4. DISCUSSION AND CONCLUSION

Our results indicate a clear increase in the stiffness of the sclera as a function of IOP. The biomechanical properties of the sclera measured in this work corroborate with the works on sclera elasticity measurements available in the literature, thus indicating the potential of OCE to assess elasticity of the sclera [37]. Our results also indicated a potential variation

in the directional assessment of elasticity, which may suggest that the sclera exhibits anisotropic biomechanical properties. Anisotropic behavior would be consistent with the regional changes in scleral ultrastructure (variable thickness and collagen fibril orientation) and subsequent biomechanical properties [17, 38].

The megapascal scale stiffness of the sclera can be a limiting factor for obtaining a detailed analysis of scleral elasticity due to the relatively high speed of the elastic wave. As such, future work will be focused on optimizing this technique to obtain a regional assessment of the biomechanical properties of the sclera as well as more detailed measurement of scleral mechanical anisotropy. Currently, the evaluation of the posterior sclera is unfeasible for *in vivo* application using the presented technique. However, advanced loading technique or even passive elastography [39] may overcome these limitations, enabling noninvasive *in vivo* assessment of scleral biomechanical properties.

ACKNOWLEDGEMENTS

REFERENCES

[1]   G. K. Lang, and O. Gareis, [Ophthalmology: A Pocket Textbook Atlas] Thieme, Stuttgart(2007).
[2]   N. A. McBrien, and A. Gentle, "Role of the sclera in the development and pathological complications of myopia," Prog Retin Eye Res*, 22(3), 307-38 (2003).
[3]   B. Coudrillier, J. K. Pijanka, J. L. Jefferys *et al.*, "Glaucoma-related Changes in the Mechanical Properties and Collagen Micro-architecture of the Human Sclera," PLoS One*, 10(7), e0131396 (2015).
[4]   J. A. Rada, S. Shelton, and T. T. Norton, "The sclera and myopia," Exp Eye Res*, 82(2), 185-200 (2006).
[5]   J. K. Pijanka, B. Coudrillier, K. Ziegler *et al.*, "Quantitative mapping of collagen fiber orientation in non-glaucoma and glaucoma posterior human sclerae," Invest Ophthalmol Vis Sci*, 53(9), 5258-70 (2012).
[6]   M. C. Leske, A. Heijl, M. Hussein *et al.*, "Factors for glaucoma progression and the effect of treatment: the early manifest glaucoma trial," Arch Ophthalmol*, 121(1), 48-56 (2003).
[7]   D. S. Schultz, J. C. Lotz, S. M. Lee *et al.*, "Structural factors that mediate scleral stiffness," Invest Ophthalmol Vis Sci*, 49(10), 4232-6 (2008).
[8]   B. Cruz Perez, J. Tang, H. J. Morris *et al.*, "Biaxial mechanical testing of posterior sclera using high-resolution ultrasound speckle tracking for strain measurements," Journal of Biomechanics*, 47(5), 1151-1156 (2014).
[9]   A. Eilaghi, J. G. Flanagan, I. Tertinegg *et al.*, "Biaxial mechanical testing of human sclera," J Biomech*, 43(9), 1696-701 (2010).
[10]   B. K. Pierscionek, M. Asejczyk-Widlicka, and R. A. Schachar, "The effect of changing intraocular pressure on the corneal and scleral curvatures in the fresh porcine eye," Br J Ophthalmol*, 91(6), 801-3 (2007).
[11]   M. J. Girard, J. K. Suh, M. Bottlang *et al.*, "Scleral biomechanics in the aging monkey eye," Invest Ophthalmol Vis Sci*, 50(11), 5226-37 (2009).
[12]   J. Tang, and J. Liu, "Ultrasonic measurement of scleral cross-sectional strains during elevations of intraocular pressure: method validation and initial results in posterior porcine sclera," J Biomech Eng*, 134(9), 091007 (2012).
[13]   C. A. Grant, N. H. Thomson, M. D. Savage *et al.*, "Surface characterisation and biomechanical analysis of the sclera by atomic force microscopy," J Mech Behav Biomed Mater*, 4(4), 535-40 (2011).
[14]   M. J. Girard, J. C. Downs, M. Bottlang *et al.*, "Peripapillary and posterior scleral mechanics--part II: experimental and inverse finite element characterization," J Biomech Eng*, 131(5), 051012 (2009).
[15]   M. J. Girard, J. K. Suh, M. Bottlang *et al.*, "Biomechanical changes in the sclera of monkey eyes exposed to chronic IOP elevations," Invest Ophthalmol Vis Sci*, 52(8), 5656-69 (2011).
[16]   R. Grytz, M. A. Fazio, M. J. Girard *et al.*, "Material properties of the posterior human sclera," J Mech Behav Biomed Mater*, 29, 602-17 (2014).
[17]   M. J. Girard, A. Dahlmann-Noor, S. Rayapureddi *et al.*, "Quantitative mapping of scleral fiber orientation in normal rat eyes," Invest Ophthalmol Vis Sci*, 52(13), 9684-93 (2011).

[18]   M. Asejczyk-Widlicka, and B. K. Pierscionek, "The elasticity and rigidity of the outer coats of the eye," Br J Ophthalmol, 92(10), 1415-8 (2008).

[19]   K. V. Larin, and D. D. Sampson, "Optical coherence elastography - OCT at work in tissue biomechanics [Invited]," Biomed Opt Express, 8(2), 1172-1202 (2017).

[20]   J. Schmitt, "OCT elastography: imaging microscopic deformation and strain of tissue," Opt Express, 3(6), 199-211 (1998).

[21]   D. V. Litwiller, S. J. Lee, A. Kolipaka et al., "MR elastography of the ex vivo bovine globe," J Magn Reson Imaging, 32(1), 44-51 (2010).

[22]   A. S. Dikici, I. Mihmanli, F. Kilic et al., "In Vivo Evaluation of the Biomechanical Properties of Optic Nerve and Peripapillary Structures by Ultrasonic Shear Wave Elastography in Glaucoma," Iran J Radiol, 13(2), e36849 (2016).

[23]   D. Huang, E. A. Swanson, C. P. Lin et al., "Optical coherence tomography," Science, 254(5035), 1178-81 (1991).

[24]   M. Sticker, C. K. Hitzenberger, R. Leitgeb et al., "Quantitative differential phase measurement and imaging in transparent and turbid media by optical coherence tomography," Opt Lett, 26(8), 518-20 (2001).

[25]   S. Wang, and K. V. Larin, "Optical coherence elastography for tissue characterization: a review," J Biophotonics, 8(4), 279-302 (2015).

[26]   S. Wang, and K. V. Larin, "Noncontact depth-resolved micro-scale optical coherence elastography of the cornea," Biomed Opt Express, 5(11), 3807-21 (2014).

[27]   C. Wu, Z. Han, S. Wang et al., "Assessing age-related changes in the biomechanical properties of rabbit lens using a coaligned ultrasound and optical coherence elastography system," Invest Ophthalmol Vis Sci, 56(2), 1292-300 (2015).

[28]   S. Wang, and K. V. Larin, "Shear wave imaging optical coherence tomography (SWI-OCT) for ocular tissue biomechanics," Opt Lett, 39(1), 41-4 (2014).

[29]   R. K. Manapuram, S. Aglyamov, F. M. Menodiado et al., "Estimation of shear wave velocity in gelatin phantoms utilizing PhS-SSOCT," Laser Physics, 22(9), 1439-1444 (2012).

[30]   M. D. Twa, J. Li, S. Vantipalli et al., "Spatial characterization of corneal biomechanical properties with optical coherence elastography after UV cross-linking," Biomed Opt Express, 5(5), 1419-27 (2014).

[31]   J. F. Doyle, [Wave Propagation in Structures Spectral Analysis Using Fast Discrete Fourier Transform] New York:Springer, (1997).

[32]   Z. Han, M. Singh, S. Aglyamov et al., "Quantifying tissue viscoelasticity using optical coherence elastography and the Rayleigh wave model," Journal of Biomedical Optics, 21(9), 090504 (2016).

[33]   M. Singh, J. Li, S. Vantipalli et al., "Noncontact Elastic Wave Imaging Optical Coherence Elastography (EWI-OCE) for Evaluating Changes in Corneal Elasticity due to Cross-Linking," Selected Topics in Quantum Electronics, IEEE Journal of, 22(3), 1-11 (2016).

[34]   Z. Han, J. Li, M. Singh et al., "Analysis of the effect of the fluid-structure interface on elastic wave velocity in cornea-like structures by OCE and FEM," Laser Physics Letters, 13(3), 035602 (2016).

[35]   Z. Han, J. Li, M. Singh et al., "Analysis of the effects of curvature and thickness on elastic wave velocity in cornea-like structures by finite element modeling and optical coherence elastography," Applied Physics Letters, 106(23), 233702 (2015).

[36]   S. Aglyamov, S. Wang, A. Karpiouk et al., "The dynamic deformation of a layered viscoelastic medium under surface excitation," Physics in Medicine and Biology, 60(11), 4295-4312 (2015).

[37]   I. A. Sigal, J. G. Flanagan, and C. R. Ethier, "Factors influencing optic nerve head biomechanics," Invest Ophthalmol Vis Sci, 46(11), 4189-99 (2005).

[38]   A. Elsheikh, B. Geraghty, D. Alhasso et al., "Regional variation in the biomechanical properties of the human sclera," Exp Eye Res, 90(5), 624-33 (2010).

[39]   T. M. Nguyen, A. Zorgani, M. Lescanne et al., "Diffuse shear wave imaging: toward passive elastography using low-frame rate spectral-domain optical coherence tomography," J Biomed Opt, 21(12), 126013 (2016).